
Article:
Muneerel-Deen Faik, A. and Zhang, Y. orcid.org/0000-0002-9736-5043 (2020) Liquid-phase dynamics during the two-droplet combustion of diesel-based fuel mixtures. Experimental Thermal and Fluid Science, 115. 110084. ISSN 0894-1777

https://doi.org/10.1016/j.expthermflusci.2020.110084

Liquid-Phase Dynamics during the Two-Droplet Combustion of Diesel-Based Fuel Mixtures

Ahmad Muneerel-Deen Faik[1,*], Yang Zhang[2]
[1] Mechanical Engineering Department, Mustansiriyah University, Baghdad, Iraq
[2] Department of Mechanical Engineering, The University of Sheffield, Sheffield, UK

Abstract

The liquid-phase processes occurring during fuel droplet combustion are important in deciding the behaviour of the overall combustion process, especially, for the binary fuel droplets. Hence, understanding these processes is essential for explaining the combustion of the binary fuel droplet. However, experimental investigation of such processes is not easily accomplishable due to the very short period of time available for tracking them within the finely small fuel droplet. In the present work, a high speed imaging and subsequent image processing leading to quantitative analysis of the binary fuel droplet combustion including liquid-phase dynamics are performed. Two categories of binary fuels – in which diesel is the base fuel – are prepared and utilized. The first category is biodiesel/diesel and bioethanol/diesel blends, while the second category is the water-in-diesel and diesel-in-water emulsions. Specific optical setup is developed and used for tracking droplet combustion. The resulting magnification of the droplet images is up to 30 times the real size, offering the possibility of droplet interior visualization at high imaging rates up (to 40000 fps). With the aid of this setup, spatial and temporal tracking of nucleation, bubble formation, puffing, microexplosion, and secondary atomization during the combustion of two adjacent binary fuel droplets are performed. The burning rate constants are evaluated and found to have the same trends as the isolated droplet combustion. However, the ratio of the droplet burning rate constant of the interactive droplet combustion to that of the isolated droplet combustion is higher than unity. This is the same for the nucleation rate within the interacting fuel droplets.

Keywords: Fuel droplet, Blends and Emulsions, Droplet liquid-phase, Nucleation, Secondary atomization.

[*] Corresponding author. Email: a.fiak@uomustansiriyah.edu.iq

1. Introduction

Droplet formation by atomization is essential in combustion applications, since the majority of the combustion systems (such as the IC engines and industrial furnaces) work on liquid fuels that cannot be used before being atomized. Additionally, higher liquid surface to mass ratio is obtained by atomization, leading to higher rates of evaporation, fuel/air mixing, and in turn, increased combustion efficiency of such systems [1]. Some of these liquid fuels are utilized in the form of fuel mixtures. This is either for increasing the performance of the combustion system by the addition of higher heating value fuels, or reducing the harmful environmental impact of the conventional fuels; or because of the depletion of the conventional fuel resources. No chemical reaction occurs between the fuel constituents in the fuel mixture, and each constituent sustains its own physical and chemical properties. Consequently, unlike the single-component (neat) fuel droplet combustion – wherein evaporation is the major rate controlling process – the droplet combustion of the fuel mixtures encompasses the effect of droplet interior heat and mass transfer [2]. As a result, the droplet combustion of the fuel mixture is much more intricate compared to the neat fuel droplet combustion. Primarily, the different boiling points and evaporation rates of the different fuel components result in concentration gradient in the droplet liquid phase. In addition, the more volatile components tend to evaporate first (because of the boiling point inconsistency) leading to the reduction in their concentrations and the variation of the concentration gradient within the droplet liquid phase. Furthermore, the evaporation process is affected by the internal circulation generated by the flow of the more volatile components towards the droplet surface and the less volatile components towards the droplet centre [3].

Accordingly, theoretical and experimental studies of the fuel mixture droplet combustion have been – and being – performed extensively aiming for deep understanding of the associated physical and chemical processes [2,4–8]. Puffing and microexplosion are among the most processes that are examined. Microexplosion is defined as the prompt fragmentation of the droplet as a result of nucleation and explosive boiling of the less boiling point component(s) [9,10]. If this fragmentation is limited and less intensive, it is commonly termed as puffing. Though, Tsue et. al. [11] and Watanbe et al., [12], specifically defined puffing as the process of vapour jet discharge form the fuel droplet surface. Occasionally, this jet is occupied by finely small sub-droplets of the dispersed phase. Ligaments and small size droplets of the continuous phase may also disintegrate from the droplet surface during intensive puffing [13]. This ligament disintegration is commonly termed *secondary atomization* [14]. The occurrence of puffing and microexplosion during the multicomponent fuel droplet combustion is firstly described by Dryer and co-workers [15–18] who described it as the *disruptive burning* of the multicomponent fuel droplets. The same has been depicted Avedisian and co-workers [19–21], Hoxie, Schoo, and Braden [8], Botero et al., [7], Segawa et al., [22] and Avulapati et. al., [23] respectively. It is found that nucleation and bubble generation inside the droplet is the prime source of disruptive burning [15,16]. Microscopic examination of the emulsion droplets before and after heating has also revealed droplet size increase due to bubble formation [24]. Microexplosion has also been attributed to the bubble formation inside burning emulsion droplets [25]. Comprehensive theoretical characterizations of bubble formation, growth, and explosion inside the liquid phase of emulsion fuel droplets are given by Shinjo et. al., [10,26,27]. Whereas, detailed experimental visualization of these processes during the combustion of an isolated fuel mixture droplet are performed by the authors in a recent article [28].

Conversely, the mutual interaction between the adjacent droplets in the liquid fuel spray is intensely affecting the ambient surrounding the droplets, and the evaporation and burning rates of each individual droplet [3]. Thus, the consideration of this interaction in the study of droplet combustion is crucially vital for spray applications. The number of droplets and the spacing distance between them represent the foremost effective parameters in this interaction. Droplet spacing distance is the net gap separating the centres of two contiguous droplets. This distance is vital in defining the flame shape and combustion behaviour of the burning droplets. Hence, there is a critical spacing distance below which the adjacent droplets are burning in one envelope flame, whereas for higher values of the spacing distance each droplet will has its own surrounding flame. The droplet spacing distance is usually normalized by – and expressed in terms of – the droplet diameter, for example, it is found that the ratio of the critical droplet spacing to the diameter of n-heptane droplets is about 17 [3]. A wide variety of research articles have been dedicated for studying the effect of droplet spacing distance on the combustion of the adjacent fuel droplets. The ignition delay time is found to decrease by increasing the spacing distance [29,30]. This is the same for the droplet burning rate [31–33], while the flame spread is increased [34]. However, Struk et al., [35] claimed that the effect of droplet spacing on the droplet burning rate is relatively less effective. Table 1 shows the regularly studied values of the droplet spacing distance normalized by its diameter with the corresponding number of burning droplets. As

the table shows, different values of spacing distance and droplet numbers are studied.

Table 1: Selected published work showing the range of droplet spacing with the number of droplets.

Work performed by	No. of Droplets	Normalized Spacing Distance
Okai et al., [32,33,36]	2	2-6
Struk et al., [35]	2	5-20
Nomura and co-workers [34,37]	10	2-12.75
Kataoka et al., [38]	13	4-35
Segawa et al., [30,39]	49	3-16

Nevertheless, the research on the interactive combustion between multiple droplets is only devoted for the above mentioned parameters, while the effect of the mutual interaction between these droplets on the physical behaviour of the droplet itself has not been well addressed, especially in the microscopic level. This in addition to the effect of the fuel mixture on the combustion behaviour of the adjacent fuel droplets, where, it is reported that the concentration of the fuel mixture has an effect of the combustion behaviour of the droplet array [40]. However, this effect is reported for the macroscopic rather than microscopic level, i.e. for the droplet and its surroundings rather than for the droplet interior or liquid phase. Therefore, a magnified examination of the droplet liquid-phase behaviour during the interactive combustion of two adjacent fuel droplets is mandatory. For that reason, the present aims to providing a detailed understanding of the liquid-phase dynamics during the combustion of two-adjacent fuel mixture droplets. This is accomplished by performing magnified high speed imaging of the droplet liquid-phase during the combustion of the adjacent droplets. The fuel mixtures implemented in the present work are diesel-based fuels. Since, diesel blending with oxygenated fuels is one of the methods used for altering the environmental side effects of the neat diesel. Alcohols are mostly added oxygenated fuels to diesel in the IC engines [41–43]. Biodiesels are currently the most attractive alternatives for diesel fuel because of their higher biodegradation, reduced toxicity, safe storage, and enhanced lubricity compared to the ordinary diesel fuels [44]. In fact, they are being progressively more used in gas turbine engines [45–47] in addition to the diesel engines [48–50]. Because of their miscibility on diesel, biodiesels are usually added to diesel in the form of blends of variable proportions and without further engine modifications [44]. Additionally, diesel-water emulsions have also been used to reduce the NOx formation [51,52]. The addition of water to diesel reduces the combustion temperature and decreases N_2 oxidation and NOx formation. Accordingly, ethanol, biodiesel, and water are the agents added to neat diesel for producing the diesel-based fuel mixtures. The difference in diesel miscibility of these three agents has also been considered during the selection criteria. Biodiesel is completely miscible in diesel, ethanol is partially miscible [41], and water is immiscible in diesel. Hence, the effect of additive miscibility on diesel is considered in the present work.

In conclusions, the main objective of the present work is exploring the effect of droplet-droplet interaction on the liquid-phase dynamics during the combustion of diesel-based mixture fuel droplet at different concentrations. This is met by the use of high speed visualization of the droplet internal part during the combustion process.

2. Experimental Work

2.1 Fuel Mixture Preparation

Water-in-diesel (WD) emulsions (where water is the dispersed phase and diesel is the continuous phase), and diesel-in-water (DW) emulsions (where diesel is the dispersed phase and water is the continuous phase) have both been prepared and tested in the present work. This is because the ratio of the densities of both the dispersed phase and the continuous phase is found to influence the rate of nucleation within the emulsions [53]. Hence, this effect is worthy further investigation in the present work. The difference between both emulsions appears in the type of emulsifying agent used for preparing the mixture. Where the component of the mixture on which the emulsifier is more soluble is the continuous phase and the other component is the dispersed phase. This solubility inclination is characterized by the Hydrophile-Lipophile Balance (HLB) number. According to this characterization, the emulsifies with $0 \leq HLB \leq 9$ are used for making WD emulsions, while those with $11 \leq HLB \leq 20$ are used for making DW emulsions [54]. Accordingly, Polysorbate 80 (HLB = 15) is used in the present work for making the DW emulsions, and Sorbitan Mono Oleate – also known as Span 80 – (HLB = 4.3) is used for making the WD emulsions in the present work. Both emulsions have been prepared in lab prior to the combustion experiments. The method followed and described by Califano, Calabria, and Massoli [55] and Jackson and Avedisian [20] has been used for the preparation. For each of the emulsions, the emulsifier is added to the continuous phase (diesel in the case of WD emulsions, and water in the case of DW emulsions) with a quantity less than 1% of the mixture volume. The emulsifier and the continuous phase are then stirred for ensuring solubility. The required quantity of the dispersed phase (water in the case of WD emulsions, and diesel in the case of DW emulsions) is then added gradually to the mixture. A 20000 rpm electric hand blender has been used for mixing the liquids for more than five minutes until a homogeneous milky white liquid is produced. Water content in both

emulsions has been fixed at 10%, 20%, and 30% of the total emulsion volume, and the remaining part is diesel. Finally, it is worthy to mention that for every new test, a new emulsion sample is prepared and tested. Hence, these samples are kept in small transparent glass containers, and during the testing period no visible changes have been observed. While, the biodiesel-in-diesel (BD) and ethanol-in-diesel (ED) blends have been prepared in-lab. For each blend, three blending proportions are used, in which diesel accounts for (90%, 80%, and 70%) of the total mixture volume, and the added fuel accounts for the remaining (10%, 20%, and 30%) respectively. These proportions are selected in accordance to those corresponding values of diesel emulsions. This ensures relatively comparable results.

2.2 Optical Setups and Testing Procedures

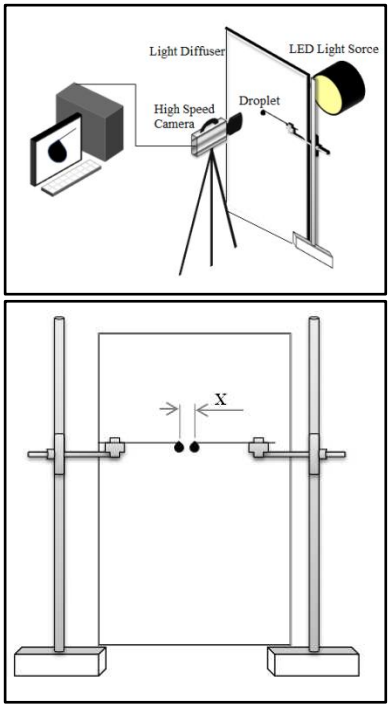

Figure 1: (a) Experimental setup of the droplet combustion with backlighting imaging, (b) neighbouring droplets suspension arrangement.

The setup used during experiments is shown in Figure 1. The droplets are oppositely suspended on two (100 µm) monofilament SiC fibres. Each of these fibres is attached onto a sliding arm of a lab stand for more efficient control of the fibre position with respect to the camera. A micro-fine syringe with hypodermic (0.33 mm) diameter and (12.7 mm) length needle was used for generating and suspending the droplets on the SiC fibres. A relatively constant amount of fuel volume is injected every time for generating and suspending the droplet on the SiC fibre. The initial diameters of all the droplets generated and adopted in experiments are evaluated using image processing and is evaluated to be 1.207±0.269 mm. Droplet ignition has been carried out using the hot wire ignition method. Hot wire ignition is widely used for igniting the droplet in experimental work, for example those carried out by [8,37,56,57]. The SiC fibre is served as the hot wire, where it is heated on the side far from the droplet suspension location. After the droplet is suspended, a butane flame is placed below the fibre 5 mm away from the droplet. This point is selected to keep the effect of the butane flame on droplet combustion to minimum. This includes preventing any form of interference between the butane flame and the flame surrounding the burning droplet. The heat generated in the zone above the flame is transferred quickly by conduction to the part suspending the droplet. This is due to the relatively high thermal conductivity of the SiC fibre. The butane flame is then removed after the droplet is ignited. The resulting ignition delay time using this method is estimated to be in the range of 150 ms. This comprises the time period from placing the flame under the fibre to the first appearance of the visible flame around the droplet. This method is found to produce a reliable and repeatable droplet ignition for all the tested fuel droplets. Droplet initial diameter is evaluated at the first image preceding the appearance of the visible flame around the droplet.

In due course, a Nikon AF micro Nikkor 60 mm f/2.8D lens with a 55 mm macro extension tube set are attached to the Photron SA4 high speed camera for making the optical setup. The camera and optical arrangement are fixed before the droplets, whereas an IDT 19-LED high intensity illuminator is installed behind the droplet serving for providing the light required for illumination. A translucent white light-diffuser is installed between the droplet and the light source for lower light intensity, and more uniform light distribution behind the droplet. Two camera settings are used in the present work. The first is used for tracking the droplet overall combustion and the surrounding flame. For these reasons, the camera is set to 1000 fps framing rate, 1 ms exposure time, and 768x768 pixels image resolution. The area covered by the camera was 7.68x7.68 mm^2, giving a spatial resolution of 30 µm/pixel for each image. The magnification rate achieved using this setup is 30 times the physical size. The second setting is used for tracking the liquid-phase of the interacting fuel droplets. Hence, the camera is set to 40000 fps framing rate, 25 µs exposure time, and 320x240 pixels image resolution. The area covered by the camera was 3.2x2.4 mm^2, giving a spatial resolution of 30 µm/pixel for each image. The normalized spacing distance is varied in a range of (1-5) to investigate its effect on the droplet combustion. The images are stored in the (TIFF)

format and processed according to specifically written Matlab algorithms. Finally, it is worthy to mention that the reference time for each of the physical processes presented in this work is the time where the process initiated throughout to the droplet lifetime, i.e. the first image is the one at which the process started, and then come the rest of images in sequence.

3. Results and Discussions

3.1 Flame Shape and Droplet Burning Rate

As explained previously, the normalized droplet spacing distance is varied over a span of (1-5). This is to compromise for the magnification rate and the imaging area. Additionally, the spacing distance is normalized by the initial diameter of the droplet, therefore, its values are almost but not exactly the same for all the tested fuel droplets, but all are within the above specified range. This is because the droplet initial diameter is changing slightly every time within a small range, and due to the delay resulting from suspending each droplet on its own fibre, these values are also slightly different.

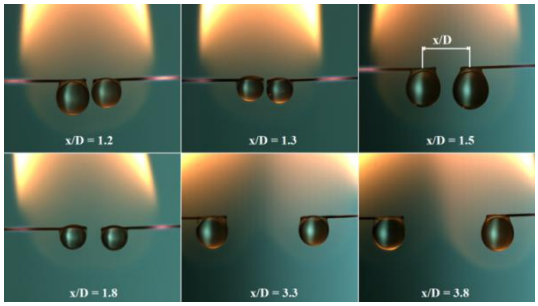

Figure 2. The effect of droplet normalized spacing distance on the flame surrounding the burning diesel fuel.

Figure 2 shows the effect of changing the normalized spacing distance on the flame surrounding the interacting neat diesel fuel droplets. The normalized droplet spacing distance is set to 1.2, 1.3, 1.5, 1.8, 3.3, and 3.8 respectively. For small distance values (less than 2), the two droplets are surrounded by a single flame, while for higher distance values, each droplet is surrounded by its own luminous flame. Each of the adjacent droplets in the cases shown in Figure 2 primarily had its own flame, and then these flames merged together into a single larger flame (for small spacing distance).

The same is shown to occur during the combustion of the biodiesel fuel droplets listed in Figure 3. The normalized spacing distance in this case was set to 1.2, 1.5, 2.7, 3, 3.4, and 3.8 respectively. For 1.2 and 1.5 spacing, the adjacent droplets are surrounded by a single flame. Whereas for higher spacing distance, the same fuel droplets have had two detached flames. For the 3.8 spacing distance, the droplet to the left did not ignite despite that its nearby droplet is already undergoing combustion. This is because the heat transferred from the burning droplet was not sufficient for creating a combustible mixture above the droplet, i.e. it was not adequate for raising the droplet surface temperature to the boiling point of the biodiesel.

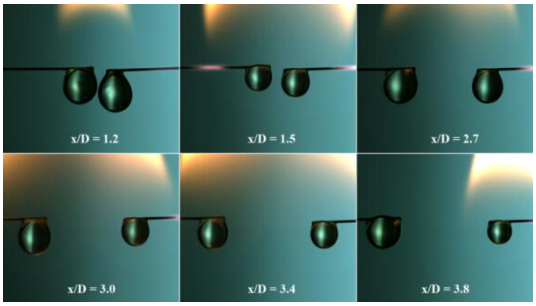

Figure 3. The interactive combustion of two-biodiesel fuel droplets at different normalized spacing distance.

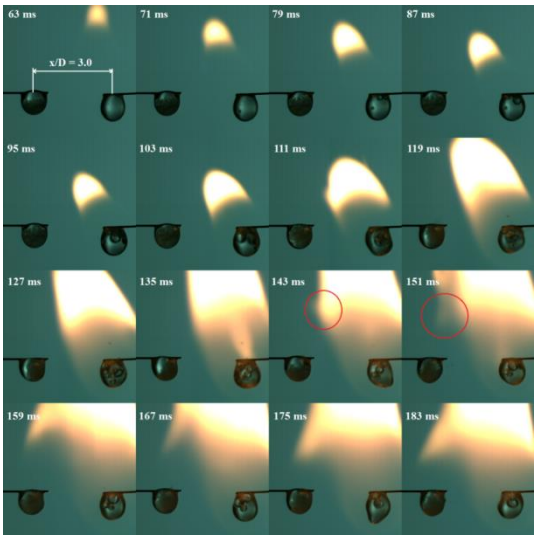

Figure 4. Temporal sequence of the flame propagation from a burning DW20 emulsion fuel droplet to its neighbour droplet.

The sequence of flame propagation from a burning fuel droplet to its adjacent unburning fuel droplet is shown in Figure 4. The droplet on the right is ignited by the hot wire ignition method. Once reached the ignition point, the fuel-vapour/air mixture above the droplet is ignited as shown in the image of time 63 ms. The flame then propagates all around the droplet as shown in images 71 ms to 119 ms respectively. In the interim, the droplet to the left – which is not ignited yet – starts heating up by the effect of convection and radiation heat transferred from the adjacent burning droplet [58]. This is depicted by comparing the liquid phase behaviour of the droplet in images 87 ms to 143 ms with those in the preceding images. The droplet surface temperature is increased by the heat received from its neighbour up until reaching the diesel boiling point. After which, fuel vapour is liberated from the droplet surface and mixed with the surrounding air forming a combustible mixture

that is ready for ignition. As soon as reaching the diesel instantaneous ignition temperature, the mixture is ignited above the droplet surface as illustrated by the red highlighting circles in images 143 ms and 151 ms. The resulting flame then propagated through the combustible mixture until the left side droplet is completely surrounded by its own flame as shown in images 159 ms to 183 ms.

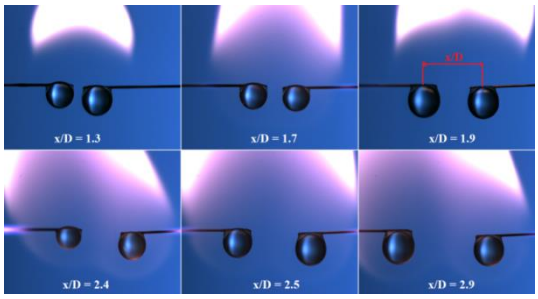

Figure 5. The effect of normalized spacing distance on the flame surrounding two interacting BD10 fuel droplets.

Figure 5 shows the interactive combustion of two BD10 fuel droplets at 1.3, 1.7, 1.9, 2.4, 2.5, and 2.9 normalized spacing distances respectively. For up to 2.5 spacing distance, a single flame is found to be surrounding the two adjacent droplets, whereas for higher spacing distance (i.e. 2.9), each droplet is surrounded by its own luminous flame. The same is noticed for the BD20 and BD30 fuel droplets. Hence, it can be suggested that for the biodiesel/diesel blends, the critical normalized spacing distance below which a single luminous flame will surround the two interacting droplets is about 3. This is to some extent dissimilar to the ethanol/diesel blends in which the two adjacent droplets are bounded by a single flame at even higher spacing distances as shown in Figure 6.

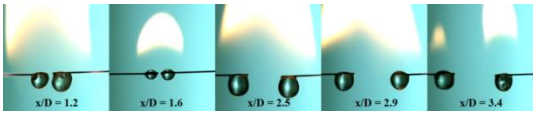

Figure 6. The interactive combustion of two-adjacent ED10 fuel droplets at different normalized spacing distance values.

Figure 6 shows two adjacent ED10 droplets at different normalized spacing distance values. The two droplets are surrounded by a single flame at distance values up to (2.9), while for the 3.4 spacing distance; each droplet had its own flame. Therefore, as stated above, it can be implied that the critical normalized spacing distance for the ethanol/diesel blends is kind of above that of the biodiesel/diesel blends. This is to some extent comparable to that of the emulsion droplets. The latter are shown to have a single flame surrounding the two neighbouring droplets at a normalized spacing distance of 3 as shown in Figure 4, and shown to have two separate flames at higher values in the case of DW20. Hence it may be conceived that the critical normalized spacing distance of the emulsion droplets is among these two magnitudes.

Figure 7 shows the effect of the spacing distance on the burning rate constant during the interactive droplet combustion of the single-component (neat) fuels, BD blends, ED blends, DW emulsions, and WD emulsions respectively. The burning rate of the multicomponent fuel droplets has been evaluated according to the same principle of the single-component fuel droplets that is by dividing the initial droplet diameter squared by the total droplet lifetime evaluated from ignition to flame extinction. Therefore, only the droplets proceeded successfully to the end are considered for evaluating droplet burning rate. That is because, in some of the multicomponent fuel droplets, especially for the water-in-diesel and diesel-in-water emulsions, the droplets go on explosion and do not proceed for complete combustion. However, in the case of diesel-in-water emulsions, for all mixture compositions, no single droplet survived to the end for complete evaporation and combustion, despite the amount of experimental tests carried out. All the droplets went on microexplosion rather than complete combustion. Accordingly, the slope of the droplet size evolution curve with time has been evaluated and assumed as the burning rate for this fuel mixture. This assumption is valid according to the D^2-model assumption of the burning rate constant being the slope of the D^2-equation relating droplet size evolution with burning time. Additionally, this method of evaluating the burning rate has been implemented by other published works for evaluating the burning rate for emulsion droplets, such as that of Wang et al., [59]. The uncertainty of burning rate values has been expressed in terms of the standard deviation (STD) for six tested droplet samples of each of the investigated fuels. The STD for the neat fuels is 0.05, 0.11, and 0.07 for diesel, biodiesel, and ethanol respectively, while, its values for the ED and BD blends are found to be in the range (0.02 and 0.12), and for the DW and DW emulsions are in the range (0.06 and 0.42) respectively. The top graph of Figure 7 represents the neat diesel, biodiesel, and ethanol burning rates. The burning rates of both diesel and biodiesel fuel droplets are proportional to the droplet spacing distance, while those of the ethanol fuel droplets are shown to be irresponsive to the normalized spacing distance. This is attributed to the increase in the projected area of the sooty flame by increasing the distance leading to increasing the effect of heat transfer by radiation and convection and in turn, rising the temperature of the surrounding environment [35].

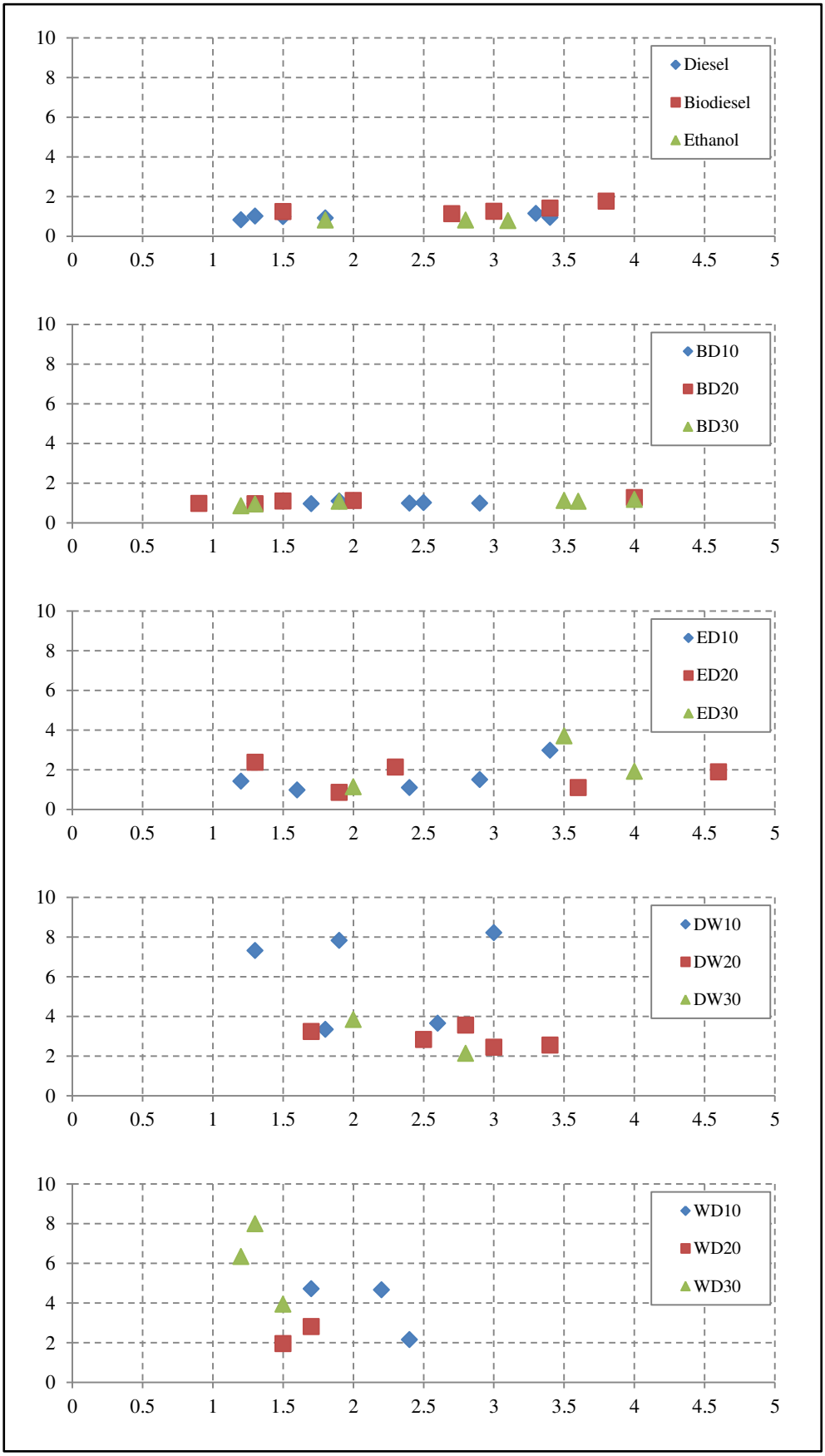

Figure 7: The effect of the normalized spacing distance (x-axis) on the average burning rate constant (mm2/s) (y-axis) during the interactive droplet combustion of all the fuels under investigation.

Additionally, the concentration gradient in the combustion zone is proportional to the normalized spacing distance [32], hence, increasing the spacing distance causes the increase in the burning rate. The burning rates of the BD blends (second graph) show a small increase with increasing the spacing distance. This increase is from 0.96 to 1.01 mm^2/s, 0.96 to 1.1711 mm^2/s, and 0.84 to 1.16 mm^2/s for spacing increase from 1.7 to 2.5, 0.9 to 4, and 1.2 to 3.5 in the cases of BD10, BD20, and BD30 blends respectively. The same trends are shown in the third graph (for the ED blends) but with higher values of the burning rate constant. A uniform distribution of the burning rate behaviour with respect to the spacing distance can be noticed for both the BD and ED blends. This distribution is not perceived in the emulsions burning rates (4^{th} and 5^{th} graphs). They are more scattered as a response to changing the spacing distance. This is shown in the case of the DW10 emulsion, where the burning rate constants at 1.8 and 2.6 spacing distance values are less than those at 1.3, 1.9, and 3.8 distance values. This in turn, makes it difficult to decide whether the burning rate is proportional or inversely proportional to the spacing distance. This is because in most cases the emulsion droplets did not undergo complete evaporation, rather, microexplosion and complete rapture of the droplets takes place in all the cases. Moreover, due to nucleation and bubble generation [28], the emulsion droplets experience size increase rather than the expected size decrease. Therefore, the evaluated burning rate constant is not accurately reflecting the burning rate of the droplet because it is expressed as the rate of change of droplet size with time. This is not the scenario for the other binary fuels, thus, the burning rate constants of these fuels exactly reflect the droplet burning rate. Furthermore, the burning rate values of Figure 7 are compared with those corresponding values of the isolated droplets listed in [60]. The difference in magnitude has been expressed in terms of the ratio of these values and is shown in Figure 8.

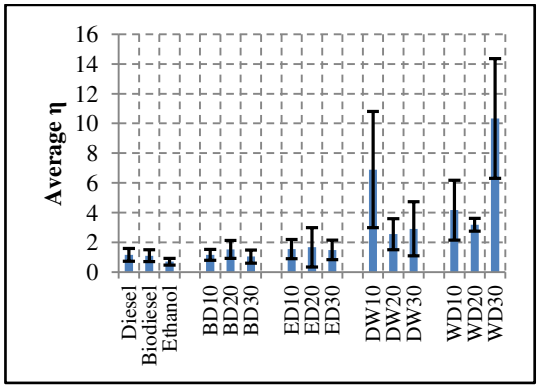

Figure 8: The ratio (η) of the burning rate constant of the interactive droplets to that of the single droplet of the same fuel averaged for all the fuels under investigation.

For neat diesel and biodiesel fuel, η is slightly higher than unity, while for ethanol, it is lower than unity. For the binary fuel mixtures, η values are all higher than unity suggesting higher burning rates of the interactive combustion of the adjacent fuel droplets compared to those of the corresponding isolated fuel droplets. Additionally, when comparing η values for the binary mixtures, the following can be inferred; the range of η for the BD blends is 1.1-1.5, giving the least values among all fuel mixtures. Next came the ED blends with 1.5-1.7 η values, whereas the DW and WD emulsions have had the highest η values ranging between 3-7 and 4-10 respectively. However, the standard deviation of the latter mixtures is relatively high for all proportions, compared to the standard deviation of the BD and ED blends in addition to the neat fuels.

3.2 Nucleation and Bubble Growth Rates

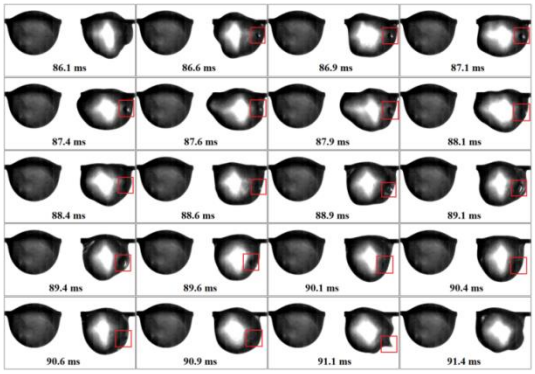

Figure 9: Temporal sequence of the bubble growth inside a WD20 droplet during the combustion of two-interactive droplets.

Figure 9 shows the temporal tracking of bubble formation and growth within WD20 droplet under interactively combustion. Bubble initiation took place in one of the droplet sides, and then due to circulation, the bubble travelled into other location. Detailed description of bubble growth can be found in [28] therefore, no further discussions will be performed on this article. However, compared to the isolated fuel droplet, the number of bubbles generated within the interacting fuel droplets is noticed to be higher. Therefore, the effect of additive concentration on the nucleation rate within the interacting binary fuel droplets is shown in Figure 10. Nucleation rate is evaluated by digitally counting the number of bubbles generated within the droplet liquid-phase during its overall lifetime. This is then averaged for the tested droplets of the same fuel mixture concentration. The algorithm used for counting the nuclei within the droplet is based on counting the objects within the image after filtering and noise removal. Then, the number of objects within the image is subtracted from that of the objects in the preceding image. From which,

the nucleation rate is obtained. Further details on the processing algorithms, procedures, and validation can be found in [60]. The standard deviation STD values of the calculated nucleation rate for the tested fuels are: 1.65, 1.07, and 0.97 for BD10, BD20, and BD30; 1.57, 1.84, and 1.89 for ED10, DE20, and ED30; 2.67, 1.03, and 1.37 for WD10, WD20, and WD30; and 2.63, 2.55, and 1.40 for DW10, DW20, and DW30 respectively.

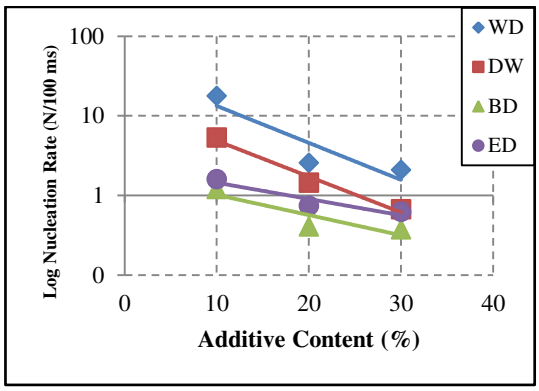

Figure 10: Average nucleation rate with respect to the concentration of the substance added to diesel in the binary fuels during the combustion of two interacting fuel droplets.

Logarithmic format is used for presenting the nucleation rate because of the large variation between the different mixtures. As shown in the figure, the nucleation rate for all the fuel mixtures is inversely proportional with the additive concentration (biodiesel, ethanol, or water). Additionally, both the WD and DW emulsion droplets have experienced the uppermost nucleation rates, followed by the ED blends, while the BD blends are the lowermost. Once more, the miscibility of the additive on diesel is the main cause of such behaviour. Biodiesel is completely miscible in diesel resulting the most stable mixture compared to other mixtures, and in accordance, the lowermost nucleation rate. Since nucleation occurs due to separation and superheat boiling of the low boiling point components [60]. Furthermore, to compare the nucleation rate within the binary droplets during both isolated combustion and interactive combustion conditions, the ratio of the latter to the former has been evaluated and presented in Figure 11 with respect to the concentration of both water and ethanol on the left side, and water and biodiesel on the right side. The nucleation rate is defined as the number of nuclei per unit time within the droplet volume [9]. The nucleation rate of the isolated fuel droplet combustion for the mixtures under investigation is available in [60]. In order to illustrate the similarity in behaviours, the WD emulsions and ED blends are presented together, while the DW emulsions and BD blends are plotted together. As the figure shows, apart from the DW10, DW20, and WD20 mixtures, the nucleation rate within the interacting fuel droplets is higher than that within the corresponding isolated fuel droplets. This is imputed to the higher heat transfer rates to the droplet from the neighbouring droplet and its surrounding flame. This in turn increases the temperature of the liquid-phase of the droplet and increases the superheat boiling of the low boiling point components in the mixtures, leading to augmenting the nucleation sites and nucleation rate in the droplet interior. Though, the different behaviour shown in the aforementioned three mixtures could be attributed to the short lifetime due to rapid disruption of the droplets of these mixtures. This in turn leads to insufficient time for nucleation. However, this might be further investigated for more in depth explanation.

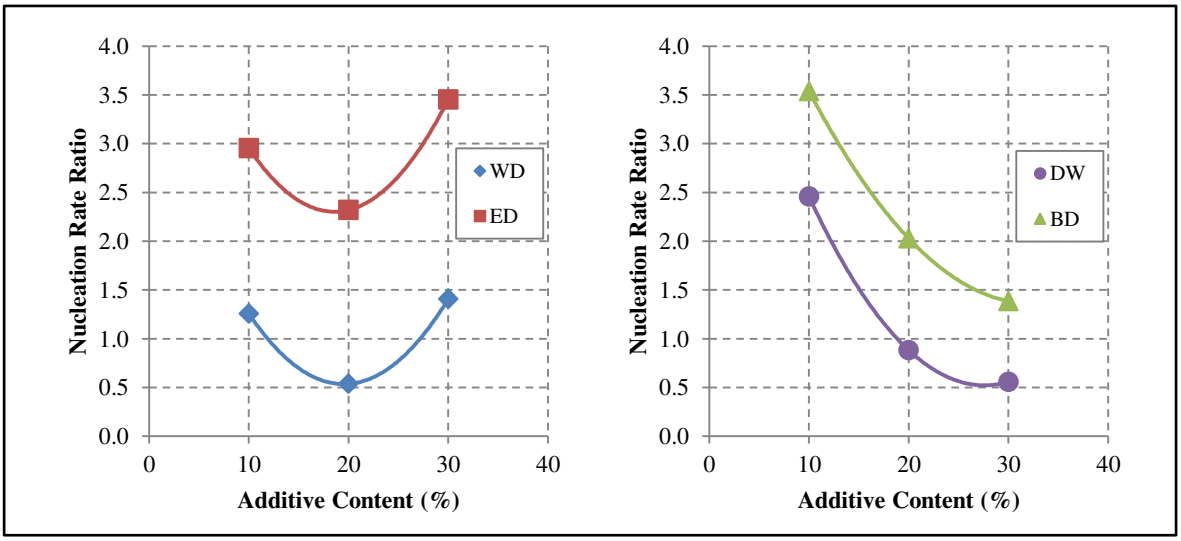

Figure 11: The effect of additive concentration on the ratio of the average nucleation rate evaluated for the two-interacting fuel droplets to that evaluated to the single isolated fuel droplet.

Additionally, it can be seen from the figure that even the BD blends which are the least in nucleation rate are experiencing an increase in the nucleation rate during the two-droplet interactive combustion. This increase may reach up to more than three times the rates of the isolated droplet as shown in the case of BD10 fuel blend. These high ratio magnitudes of the BD blends and also the ED blends are due to the lower nucleation rates of these fuels in the isolated droplet case, hence, the denominator is relatively small. This is exactly the inverse in the case of emulsions, thus, the ratio slightly (>1) in most of the cases except the DW10 case in which the ratio is up to (2.5).

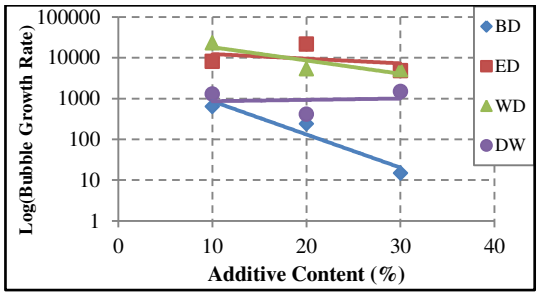

Figure 12: The effect of additive concentration on the average bubble growth rate during the combustion of two-interacting fuel droplets.

Figure 12 shows the average bubble growth rate (in logarithmic format) with respect to additive concentration within the binary fuel droplets. The growth rate is expressed in ($\mu m^3/\mu s$). It can be seen that the highest growth rates belong to the WD emulsions and ED blends, while the BD blends and the DW emulsions have experienced the lowest growth rates. This is in agreement with the nucleation rate behaviours shown in Figure 10. The uncertainty in growth rate is expressed in terms of the standard deviation (STD) of the average growth rate within three droplets for each of the tested mixtures. Table 1 shows the STD values for these mixtures.

Table 1: STD values for the bubble growth rate in Figure 12

BD10	857	**WD10**	13245
BD20	186	**WD20**	3235
BD30	2.9	**WD30**	597
ED10	12472	**DW10**	1256
ED20	31253	**DW20**	583
ED30	511	**DW30**	445

3.3 Secondary Atomization and Micro-Explosion

The adjacent droplets may experience different forms of interaction. These include thermal interaction (as shown in the rise in transfer rates between the two droplets), partaking the same flame (as for the small size droplets), and the collision and coalescence of these droplets in the form of the dynamic interaction. Keeping in mind the fact that the main feature of the binary fuel droplet combustion is the increased secondary atomization rates [28,61]. Henceforth, the effect of secondary atomization from one droplet on its neighbour droplet(s) could be worthy further considerations.

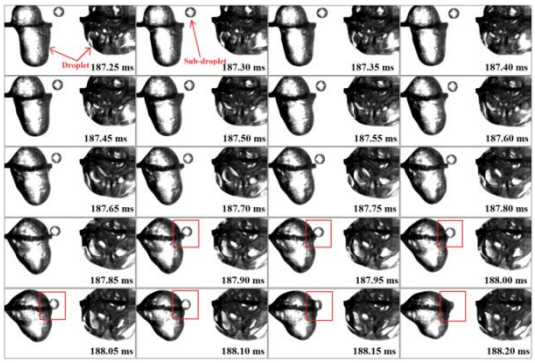

Figure 13: Temporal sequence of WD10 droplet merging with a sub-droplet emitted from a neighbouring parent droplet.

Figure 13 shows the progressive sequence of the sub-droplet collision and fusion from a burning WD10 fuel droplet (on the right) to its neighbouring droplet (on the left). Images corresponding to time 187.25 to 187.85 ms show the sequence of sub-droplet ejection and travel from the droplet on the right towards the droplet on the left. The sub-droplet touches and collides with the left droplet leading to a form of between them coalescence as shown by the red highlighting box in image 187.90 ms and the subsequent ones. Due to this coalescence, the left droplet experiences a form of size and mass increase in addition to shape variation. This shape variation is attributed to the response to the collision occurred by the relatively fast moving sub-droplet as shown in image 188.20 ms. Hence, it can be deduced that this form of interaction between the neighbouring droplets (which is not experienced by the isolated droplets) is influential in the nature of the binary fuel droplet combustion. One more form of droplet-droplet interaction is revealed in the influence of droplet microexplosion on its neighbour droplet as shown in Figure 14. Bubble burst inside the left-side droplet resulted in droplet explosion. The sequence of this burst and its subsequent effects are further explained in [28]. Images 0.03 ms and 0.13 ms show the radial travel of the explosion wave from the bursting droplet (on the left) to the adjacent droplet (on the right). When hitting the right droplet, the effect of the wave on the droplet took the form of impact-like disturbance on the droplet side facing the wave as shown in images 0.13 ms to 0.38 ms. Subsequent to the impact, the right side droplet went on partial disintegration leading to

sub-droplet ejection and secondary atomization as shown in image 0.50 ms and the consequent images. Hence, the effect of microexplosion is not limited to the bursting droplet, instead, it exceeds to the adjacent droplets leading to droplet disintegration and secondary atomization.

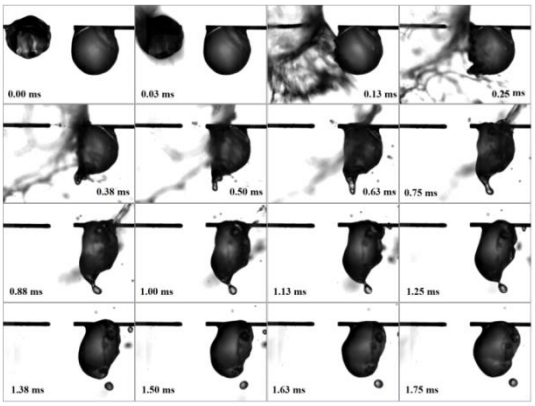

Figure 14: Temporal sequence of the effect of WD10 droplet explosion on the droplet neighbouring it (the time is set from the start of explosion).

3.4 Other Liquid Phase Dynamics

Figure 15 shows water accumulation inside the two-interacting WD10 fuel droplets. This water resulted from the separation of the emulsion mixture, and it plays the role of heterogeneous nucleation source as shown in by the growing bubble in the red bounding boxes. This accumulation occurred mostly within the WD and DW emulsions in addition to the ED blends (diesel in this case), but never happened in the BD blends.

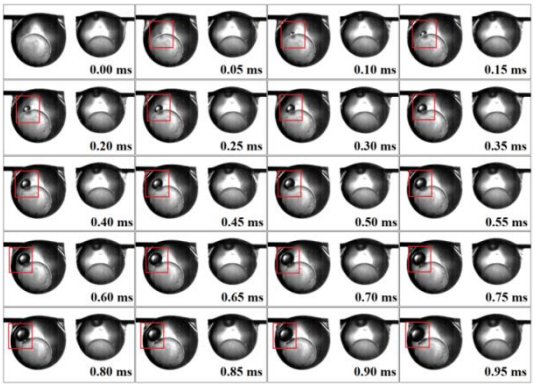

Figure 15: Temporal sequence of the effect of water agglomeration on the nucleation and bubble growth within a WD10 droplet.

This is because of the effect of miscibility difference of these agents in diesel as explained previously. This accumulation takes place due to separation of the constituents of binary fuel due to boiling point variation. The component with lower volatility will accumulate in the centre of the droplet. It can be seen from the figure that the growth time of the bubble generated on the water mass is about 0.95 ms which is relatively short period, this implies that the accumulation of water – or diesel in the ED blend – enhances bubble growth rate, and in turn, the subsequent dynamics such as puffing and secondary atomization.

Figure 16 shows the local and instantaneous soot aggregation on one side of a burning neat diesel fuel droplet during the interactive combustion of two adjacent diesel fuel droplets. Soot formation around the isolated burning droplet is visualized and approved by a number of researchers under microgravity conditions [21,62,63]. The soot particles travel from the flame towards the droplet in the form of a cloud of black particles rather than a bulk or rigid body [63]. This is the same description of the mass bounded by the red square in Figure 16. Though, in the present work, the high magnification rate of the optical setup in addition to the steady burning of the neat diesel fuel droplet compared to that of the binary fuel droplets made it easy to track and visualize any flow inside and around the droplet including soot formation. Once formed, the soot aggregated on the outer side of the right-side droplet as shown in images 0.75 ms to 11.25 ms. Soot aggregation on this side occurred because it represents the boundary of the flame surrounding both droplets; hence, soot aggregation on the intermediate part between the two droplets is not possible. Thereafter, the soot moved upwards due to the buoyancy effect as shown in images 5.25 ms to 11.25 ms. The upward motion of the soot takes the form of a vortex as shown in the figure. This suggests the existence of such vortices around the burning droplet.

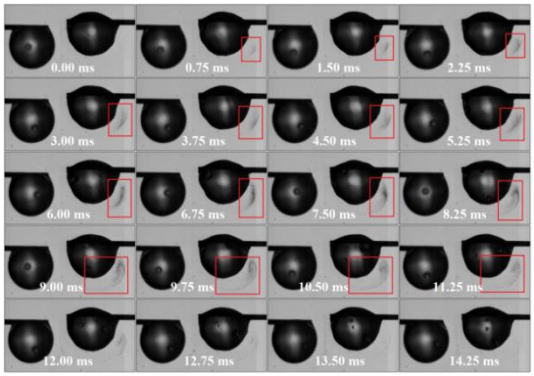

Figure 16: Temporal sequence of the soot aggregation around a burning diesel fuel droplet (the time is set from the appearance of the soot).

4. Conclusions

In the present work, the liquid-phase of the binary fuel in addition to the neat-base fuel droplet has been investigated during the interactive combustion of two-adjacent droplets. Magnified high speed imaging has been implemented in the work. The effect of mutual interaction of the droplets on the burning rate constant and flame shape have been examined initially. Then, the effect

of this interaction on the nucleation and bubble generation in the droplet liquid-phase has been investigated. The following main points are concluded:

- The critical normalized spacing distance below which the two adjacent droplets will be surrounded by a single flame is estimated to be around 3 in the case of the biodiesel/diesel blends and to some extent higher for each of the ethanol/diesel blends, water-in-diesel emulsions, and diesel-in-water emulsions.
- For all the binary fuel mixtures, the nucleation rate is inversely proportional to the additive concentration (biodiesel, ethanol, or water). Additionally, the droplets of both emulsions had the highest nucleation rates, then the ethanol/diesel blends, and the lowest were the biodiesel/diesel blends. This is attributed to the miscibility of these additives to diesel.
- Compared to the corresponding isolated fuel droplets, the nucleation rate in the interacting fuel droplets is higher. This is attributed to the increased heat transfer rates to the droplet from the flame and neighbouring droplet [58].
- Except the diesel-in-water emulsion, the bubble growth rate is inversely proportional to the increase in additive concentration. Additionally, the water-in-diesel emulsions and ethanol/diesel blends have the uppermost growth rates, while biodiesel/diesel blends and diesel-in-water emulsions had the lowermost growth rates respectively.
- The secondary atomization of the burning droplet is highly affected by the secondary atomization and microexplosion from its neighbouring droplet.
- Furthermore, separation and accumulation of the less volatile component (diesel in the ethanol/diesel blends, and water in the water-in-diesel and diesel-in-water emulsions) in the binary fuel droplets has also been observed.

5. Acknowledgement

The first author is obliged to the scholarship awarded by the Higher Committee for Education Development (HCED) in Iraq.

6. References

[1] Lefebvre, A.H. "*Atomization and Sprays.*" Hemisphere Publishing Corporation; 1989.

[2] Wang, C. H., Liu, X. Q., Law, C.K. "*Combustion and Microexplosion of Freely Falling Multicomponent Droplets.*" Combustion and Flame 1984;56:175–97.

[3] Siringnano, W.A. "*Fluid Dynamics and Transport of Droplets and Sprays.*" 2nd Editio. Cambridge University Press; 2010.

[4] Wood, B. J., Wise, H., Inami, S.H. "*Heterogeneous Combustion of Multicomponent Fuels.*" Combustion and Flame 1960;4:235–42.

[5] Niioka, T., Sato, J. "*Combustion and Microexplosion Behavior of Miscible Fuel Droplets under High Pressure.*" Symposium (International) on Combustion/The Combustion Institute 1986;21:625–31.

[6] Takei, M., Tsukamoto, T., Niioka, T. "*Ignition of Blended-Fuel droplet in High-Temperature Atmosphere.*" Combustion and Flame 1993;93:149–56.

[7] Botero, M. L., Huang, Y., Zhu, D. L., Molina, A., Law, C.K. "*Synergistic Combustion of Droplets of Ethanol, Diesel and Biodiesel Mixtures.*" Fuel 2012;94:342–7.

[8] Hoxie, A., Schoo, R., Braden, J. "*Microexplosive Combustion Behavior of Blended Soybean Oil and Butanol Droplets.*" Fuel 2014;120:22–9.

[9] Mikami, M., Yagi, T., Kojima, N. "*Occurrence Probability of Microexplosion in Droplet Combustion of Miscible Binary Fuels.*" Symposium (International) on Combustion/The Combustion Institute 1998;27:1933–41.

[10] Shinjo, J., Xia, J., Ganippa, L.C., Megaritis, A. "*Physics of Puffing and Microexplosion of Emulsion Fuel Droplets.*" Physics of Fluids 2014;26:103302.

[11] Tsue, M., Segawa, D., Kadota, T., Yamasaki, H. "*Observation of Sooting Behavior in an Emulsion Droplet Flame by Planar Laser Light Scattering in Microgravity.*" Symposium (International) on Combustion/The Combustion Institute 1996;26:1251–8.

[12] Watanabe, H., Harada, T., Matsushita, Y., Aoki, H., Miura, T. "*The Characteristics of Puffing of the Carbonated Emulsified Fuel.*" International Journal of Heat and Mass Transfer 2009;52:3676–84.

[13] Miglani, A., Basu, S., Kumar, R. "*Insight into Instabilities in Burning Droplets.*" Physics of Fluids 2014;26.

[14] Wang, Z.G. "*Internal Combustion Processes of Liquid Rocket Engines: Modeling and Numerical Simulations.*" John Wiley and Sons Ltd.; 2016.

[15] Lasheras, J. C., Fernandez-Pello, A. C., Dryer, F.L. "*Experimental Observations on the Disruptive Combustion of Free Droplets of Multicomponent Fuels.*" Combustion Science and Technology 1980;22:195–209.

[16] Lasheras, J. C., Fernandez-Pello, A. C., Dryer, F.L. "*On the Disruptive Burning of Free Droplets of Alcohol/n-Paraffin*

Solutions and Emulsions." Symposium (International) on Combustion/The Combustion Institute 1981;18:293–305.

[17] Yap, L., Kennedy, I. M., Dryer, F.L. "*Disruptive and Micro-Explosive Combustion of Free Droplets in Highly Convective Environments.*" Combustion Science and Technology 1984;41:291–313.

[18] Lasheras, J. C., Yap, L. T., Dryer, F.L. "*Effect of the Ambient Pressure on the Explosive Burning of Emulsified and Multicomponent Fuel Droplets.*" Symposium (International) on Combustion / The Combustion Institute 1984;20:1761–72.

[19] Yang, J. C., Avedisian, C.T. "*The Combustion of Unsupported Heptane/Hexadecane Mixture Droplets at Low Gravity.*" Symposium (International) on Combustion/The Combustion Institute 1988;22:2037–44.

[20] Jackson, G. S., Avedisian, C.T. "*Combustion of Unsupported Water-in-n-Heptane Emulsion Droplets in a Convection-Free Environment.*" International Journal of Heat and Mass Transfer 1998;41:2503–15.

[21] Liu, Y. C., Avedisian, C.T. "*A Comparison of the Spherical Flame Characteristics of Sub-Millimeter Droplets of Binary Mixtures of n-Heptane/Iso-Octane and n-Heptane/Toluene with a Commercial Unleaded Gasoline.*" Combustion and Flame 2012;159:770–83.

[22] Segawa, D., Yamasaki, H., Kadota, T., Tanaka, H., Enomoto, H., Tsue, M. "*Water-Coalescence in an Oil-in-Water Emulsion Droplet Burning under Microgravity.*" Proceedings of the Combustion Institute 2000;28:985–90.

[23] Avulapati, M. M., Ganippa, L. C., Xia, J., Megaritis, A. "*Puffing and Micro-Explosion of Diesel-Biodiesel-Ethanol Blends.*" Fuel 2016;166:59–66.

[24] Chung, S. H., Kim, J.S. "*An Experiment on Vaporization and Microexplosion of Emulsion Fuel Droplets on a Hot Surface.*" Symposium (International) on Combustion / The Combustion Institute 1990;23:1431–5.

[25] Tsue, M., Yamasaki, H., Kadota, T., Segawa, D., Kono, M. "*Effect of Gravity on Onset of Microexplosion for an Oil-in-Water Emulsion Droplet.*" Symposium (International) on Combustion/The Combustion Institute 1998;27:2587–93.

[26] Shinjo, J., Xia, J. "*Combustion Characteristics of a Single Decane/Ethanol Emulsion Droplet and a Droplet Group under Puffing Conditions.*" Proceedings of the Combustion Institute 2017;36:2513–21.

[27] Shinjo, J., Xia, J., Ganippa, L. C., Megaritis, A. "*Puffing-Enhanced Fuel/Air Mixing of an Evaporating n-Decane/Ethanol Emulsion Droplet and a Droplet Group under convective heating.*" Journal of Fluid Mechanics 2016;793:444–76.

[28] Faik, A.M.D., Zhang, Y. "*Multicomponent fuel droplet combustion investigation using magnified high speed backlighting and shadowgraph imaging.*" Fuel 2018;221:89–109.

[29] Sangiovanni, J. J., Kesten, A.S. "*Effect of Droplet Interaction on Ignition in Monodispersed Droplet Streams.*" Symposium (International) on Combustion/The Combustion Institute 1977;16:577–92.

[30] Segawa, D., Yoshida, M., Nakaya, S., Kadoka, T. "*Effects of Spacing and Arrangement of Droplet on Combustion Characteristics of Monodispersed Suspended-Droplet Cluster Model under Microgravity.*" Microgravity Science and Technology 2005;17:23–30. doi:10.1007/BF02872084.

[31] Koshland, C. P., Bowman, C.T. "*Combustion of Monodisperse Droplet Clouds in a Reactive Environment.*" Symposium (International) on Combustion/The Combustion Institute 1984;20:1799–807.

[32] Okai, K., Tsue, M., Kono, M., Mikami, M., Sato, J., Dietrich, D. L., Williams, F.A. "*Strongly Interacting Combustion of Two Miscible Binary-Fuel Droplets at High Pressure in Microgravity.*" Symposium (International) on Combustion/The Combustion Institute 1998;27:2651–7.

[33] Okai, K., Moriue, O., Araki, M., Tsue, M., Kono, M., Sato, J., Dietrich, D. L., Williams, F.A. "*Pressure Effects on Combustion of Methanol and Methanol/Dodecanol Single Droplets and Droplet Pairs in Microgravity.*" Combustion and Flame 2000;121:501–12.

[34] Nomura, H., Iwasaki, H., Suganuma, Y., Mikami, M., Kikuchi, M. "*Microgravity Experiments of Flame Spreading Along a Fuel Droplet Array in Fel Vapor-Air Mixture.*" Proceedings of the Combustion Institute 2011;33:2013–20.

[35] Struk, P. M., Dietrich, D. L., Ikegami, M., Xu, G. "*Interacting Droplet Combustion under Conditions of Extinction.*" Proceedings of the Combustion Institute 2002;29:609–15.

[36] Okai, K., Moriue, O., Araki, M., Tsue, M., Kono, M., Sato, J., Dietrich, D. L.,

Williams, F.A. "*Combustion of Single Droplets and Droplet Pairs in a Vibrating Field under Microgravity.*" Proceedings of the Combustion Institute 2000;28:977–83.

[37] Nomura, H., Takahashi, H., Suganuma, Y., Kikuchi, M. "*Droplet Ignition Behavior in the Vicinity of the Leading Edge of a Flame Spreading along a Fuel Droplet Array in Fuel-Vapor/Air Mixture.*" Proceedings of the Combustion Institute 2013;34:1593–600.

[38] Kataoka, H., Yamashita, H., Tada, J., Oka, Y., Morinaga, Y., Itai, M., Segawa, D., Kadota, T. "*Autoignition Behavior of a Spherical Cluster Consisted of a Center Fine Droplet and Surrounding Twelve Fine Droplets.*" Proceedings of the Combustion Institute 2015;35:1629–37.

[39] Segawa, D., Yoshida, M., Nakaya, S., Kadota, T. "*Autoignition and Early Flame Behavior of a Spherical Cluster of 49 Monodispersed Droplets.*" Proceedings of the Combustion Institute 2007;31:2149–56.

[40] Jeong, I. C., Lee, K.H. "*Auto-Ignition and Micro-Explosion Behaviors of Droplet Arrays of Water-in-Fuel Emulsion.*" International Journal of Automotive Technology 2008;9:735–40.

[41] Rakopoulos, D. C., Rakopoulos, C. D., Kakaras, E. C., Giakoumis, E.G. "*Effects of Ethanol-Diesel Fuel Blends on the Performance and Exhaust Emissions of Heavy Duty DI Diesel Engine.*" Energy Conversion and Management 2008;49:3155–62.

[42] Tutak, W., Lukács, K. Szwaja, S., Bereczky, Á. "*Alcohol-Diesel Fuel Combustion in the Compression Ignition Engine.*" Fuel 2015;154:196–206.

[43] Datta, A., Mandal, B.K. "*Impact of Alcohol Addition to Diesel on the Performance Combustion and Emissions of a Compression Ignition Engine.*" Applied Thermal Engineering 2016;98:670–82.

[44] Benjumea, P., Agudelo, J., Agudelo, A. "*Basic Properties of Palm Oil Biodiesel-Diesel Blends.*" Fuel 2008;87:2069–75.

[45] Pucher, G., Allan, W., LaViolette, M., Poitras, P. "*Emissions from a Gas Turbine Sector Rig Operated with Synthetic Aviation and Biodiesel Fuel.*" Journal of Engineering for Gas Turbines and Power 2011;133:111502(8).

[46] Chiaramonti, D., Rizzo, A. M., Spadi, A., Prussi, M., Riccio, G., Martelli, F. "*Exhaust Emissions from Liquid Fuel Micro Gas Turbine Fed with Diesel Oil, Biodiesel and Vegetable Oil.*" Applied Energy 2013;101:349–56.

[47] Kurji, H., Valera-Medina, A., Runyon, J., Giles, A., Pugh, D., Marsh, R., Cerone, N., Zimbardi, F., Valerio, V. "*Combustion Characteristics of Biodiesel Saturated with Pyrolysis Oil for Power Generation in Gas Turbines.*" Renewable Energy 2016;99:443–51.

[48] Habibullah, M., Masjuki, H. H., Kalam, M. A., Rizwanul Fattah, I. M., Ashraful, A. M., Mobarak, H.M. "*Biodiesel Production and Performance Evaluation of Coconut, Palm and their Combined Blend with Diesel in a Single-Cylinder Diesel Engine.*" Energy Conversion and Management 2014;87:250–7.

[49] Yasin, M. H. M., Paruka, P., Mamat, R., Yusop, A. F., Najafi, G., Alias, A. "*Effect of Low Proportion Palm Biodiesel Blend on Performance, Combustion and Emission Characteristics of a Diesel Engine.*" Energy Procedia 2015;75:92–8.

[50] Ileri, E., Atmanli, A., Yilmaz, N. "*Comparative Analyses of n-Butanole-Rapeseed Oil-Diesel Blend with Biodiesel, Diesel and Biodiesel-Diesel Fuels in a Turbocharged Direct Injection Diesel Engine.*" Journal of the Energy Institute 2016;89:586–93.

[51] Maiboom, A., Tauzia, X. "*NOx and PM Emissions Reduction on an Automotive HSDI Diesel Engine with Water-in-Diesel Emulsion and EGR: An Experimental Study.*" Fuel 2011;90:3179–92.

[52] Ithnin, A. M., Ahmad, M. A., Bakar, M. A. A., Rajoo, S. Yahya, W.J. "*Combustion Performance and Emission Analysis of Diesel Engine Fuelled with Water-in-Diesel Emulsion Fuel Made from Low-Grade Diesel Fuel.*" Energy Conversion and Management 2015;90:375–82.

[53] Roesle, M. L., Kulacki, F.A. "*Boiling Heat Transfer in Dilute Emulsions.*" Springer; 2013.

[54] Mollet, H., Grubenmann, A. "*Formulation Technology: Emulsions, Suspensions, Solid Forms.*" Wiley-VCH; 2001.

[55] Califano, V., Calabria, R., Massoli, P. "*Experimental Evaluation of the Effect of Emulsion Stability on Micro-Explosion Phenomena for Water-in-Oil Emulsions.*" Fuel 2014;117:87–94.

[56] Bae, J. H., Avedisian, C.T. "*High-Pressure Combustion of Submillimeter-Sized Nonane Droplets in a Low Convection Eenvironment.*" Combustion and Flame 2006;145:607–20.

[57] Ghamari, M., Ratner, A. "*Combustion Characteristics of Diesel and Jet-A Droplets Blended with Polymeric Additive.*" Fuel 2016;178:63–70.

[58] Mikami, M., Kato, H., Sato, J., Kono, M.

"*Interactive Combustion of Two Droplets in Microgravity.*" Symposium (International) on Combustion/The Combustion Institute 1994;25:431–8.

[59] Wang, C. H., Pan, K. L., Ueng, G. J., Kung, L. J., Yang, J.Y. "*Burning Behaviors of Collision-Merged Water/Diesel, Methanol/Diesel, and Water+Methanol/Diesel Droplets.*" Fuel 2013;106:204–11.

[60] Faik, A.M.D. Quantitative Investigation of the Multicomponent Fuel Droplet Combustion Using High Speed Imaging and Digital Image Processing. The University of Sheffield, 2017.

[61] Faik, A.M.E.D., Zhang, Y., Hanriot, S. de M. "*Droplet Combustion Characteristics of Biodiesel–Diesel Blends using High Speed Backlit and Schlieren Imaging*." Heat Transfer Engineering 2018;7632:1–14.

[62] Jackson, G. S., Avedisian, C. T., Yang, J.C. "*Observations of Soot during Droplet Combustion at Low Gravity: Heptane and Heptane/Monochloroalkane Mixtures.*" International Journal of Heat and Mass Transfer 1992;35:2017–33.

[63] Choi, M. Y., Lee, K.O. "*Investigation of Sooting in Microgravity Droplet Combustion.*" Symposium (International) on Combustion/The Combustion Institute 1996;26:1243–9.